Polarimetric Differential-TomoSAR Imaging

Fabrizio Lombardini, Matteo Pardini[1], Francesco Cai
Department of Information Engineering, University of Pisa, Italy

Abstract

Recently, in parallel to the maturation of the operative InSAR techniques based on phase-only data, much interest has grown in techniques based on the coherent combination of SAR images at the complex (amplitude and phase) data level, for the extraction of more rich information on the observed scene. In particular Tomographic SAR techniques constitute the frontier of this research area. Recently, the Differential Tomography framework has also been introduced and experimented, producing 'space-time' signatures of multiple non stationary scatterers superimposed in a SAR cell. To further increase the amount of information which can be extracted, in this work we extend the Differential Tomography framework in a polarimetric sense, allowing the extraction of joint information about the heights, the deformation velocities and the scattering mechanisms characterizing the imaged scatterers. First real data samples are presented of the new Polarimetric Differential Tomography concept.

1   Introduction

In the last decade, starting with Polarimetric Interferometry [1], algorithms of coherent SAR data combination have gained increasing attention in the SAR community. Exploiting the existing SAR data archives, they allow extracting rich information about the observed scene. Among these techniques, 3-D SAR Tomography (Tomo-SAR) is an experimental multibaseline (MB) interferometric mode achieving full 3-D images in the range-azimuth-height space through elevation beam forming, i.e. spatial (baseline) spectral estimation [2]. Thanks to Tomo-SAR, the resolution of multiple scatterers is made possible in height in the same layover cell, overcoming a limitation of the conventional InSAR processing. As a consequence, Tomo-SAR can add more features for the analysis of complex scenarios, e.g. for the estimation of forest height and biomass, sub-canopy topography, soil humidity and ice thickness monitoring, and extraction of heights and reflectivities in layover urban areas [3-5]. In order to retrieve information on the nature of the imaged scatterers, Tomo-SAR has also been extended to PolTomo-SAR [6]. It jointly exploits MB SAR data acquired with different polarization channels to improve the accuracy of the estimation of the vertical position of the imaged scatterers, and to estimate a set of normalized complex coefficients characterizing the corresponding polarimetric scattering mechanism.

On the other hand, multitemporal (typically MB) data, especially from spaceborne sensors, are routinely exploited by Differential InSAR methods [7-8], allowing monitoring of deformation motions (e.g. subsidences) even with millimeter accuracy on Permanent Scatterers [7]. Recently, the Differential InSAR and TomoSAR concepts have been deeply integrated to furnish a new coherent data combination framework, termed Differential Tomography (Diff-Tomo) [9]. Diff-Tomo allows the joint resolution in an elevation-deformation velocity domain of multiple superimposed scatterers mapped in a SAR cell. The concept has been demonstrated extensively with spaceborne data over urban areas with layover discrete scatterers [10-11].

In this work, a way to exploit multitemporal-MB data with polarization diversity is proposed, introducing a polarimetric extension of the Diff-Tomo framework (Pol-Diff-Tomo). This new coherent SAR data combination mode is another step in the development sequence of Tomo-, PolTomo-, and Diff-Tomo SAR processing. The new concept aims to provide the total polarimetric power distribution of the scattering in the height-deformation velocity plane and to estimate the complex polarization signature as a function of height and velocity. It is expected that this kind of analysis may improve height and deformation velocity accuracies of Diff-Tomo, furnish information on the nature of the multiple deformating scatterers at different heights interfering in the same cell, and allow identifying spurious scattering mechanisms, especially in urban environments. Here, a first Pol-Diff-Tomo processor is also proposed for the new extended Diff-Tomo mode. Moreover, first experimental results are reported of the application of the polarimetric Diff-Tomo processing to real airborne P-band data, also including a synthetic injected subsidence motion, so proving the concept.

[1] Now with the Deutsches Zentrum für Luft- und Raumfahrt (DLR), Microwave and Radar Institute, Oberpfaffenhofen (Germany).

2 The Pol-Diff-Tomo Framework

In the single polarization Diff-Tomo framework, it is assumed as a general case to process the data from N_P passes of the SAR platform with N_C phase centres for each pass (multistatic acquisition; $N_C = 1$ for the classical monostatic case) [9]. As usual in SAR interferometry, we can consider M complex looks, e.g. multiple homogeneous adjacent pixels, to reduce statistical variations. For each m-th look, the complex amplitudes of the corresponding pixels observed in the $N_C \times N_P$ images at a given range-azimuth cell are arranged in a multitemporal-MB data matrix $\mathbf{Y}(m)$.

Once one of the tracks has been selected as master track, the phase variations with respect to the master can be expressed by means of the steering matrix $\mathbf{A}(h,v)$, coding the multitemporal-MB complex response to a backscattered signal component coming from height h and with line-of-sight velocity v. Each element of $\mathbf{A}(h,v)$ is a sample of a space-time harmonic with spatial frequency $\omega_S = 4\pi h/(\lambda R \sin\theta)$ and temporal frequency $\omega_T = 4\pi v/\lambda$, where λ is the radar wavelength, R is the slant range, and θ is the look angle [7,9].

Working in a polarimetric framework, the ensemble of the data matrices acquired with K different polarizations (or linear combinations of them), can be structured in a third-order tensor $\mathbf{Y}_P(m)$ with dimensions $N_C \times N_P \times K$. For instance, employing the Pauli basis we can assume $K=3$. Let $\mathbf{k}$ be the $K \times 1$ complex vector containing the normalized polarimetric scattering coefficients. Analogously to the single polarization case, the response to a scatterer with height h, line-of-sight velocity v, and polarimetric signature $\mathbf{k}$ can be coded as a third-order polarimetric multitemporal-MB steering tensor $\mathbf{B}(h,v,\mathbf{k})$.

The Pol-Diff-Tomo framework aims at obtaining estimates of the spatial-temporal spectrum of the total polarimetric power, $\hat{P}_P(h,v)$, and of the corresponding polarimetric complex scattering coefficients, $\hat{\mathbf{k}}(h,v)$. For this purpose, here we propose the use of a multidimensional filterbank approach in which the filter coefficients are designed enforcing a unit gain for a data component corresponding to the currently tuned coordinates $(h,v,\mathbf{k})$, and at the same time reducing the leakage from other components. This design criterion should lead to increased sidelobe suppression and resolution capabilities with respect to a more conventional linear analysis. Once the multidimensional filter coefficients are obtained as a function of the generic $\mathbf{k}$, $\hat{P}_P(h,v)$ and $\hat{\mathbf{k}}(h,v)$ are given by the maximization of the filter output power over $\mathbf{k}$. The solution can be achieved in closed form as a function of the multilook estimate of the covariance matrix of the polarimetric multitemporal-MB data.

3 First Experimental Results

First Pol-Diff-Tomo analyses have been started of real fully-polarimetric repeat pass P-band airborne data, acquired in the framework of the ESA project Bio-SAR-1 by the DLR E-SAR system over a forest site in Remningstorp (Sweden). 9 tracks have been processed acquired with an overall horizontal baseline of 80m. The time span is 2 months [12], and acquisition can be considered quasi-multistatic ($N_C = 3$, $N_P = 3$). Temporal decorrelation is mild and expected detectable motions are null, which is useful for a first check of the results.

The point spread function (PSF) in the height-deformation velocity plane, corresponding to the multitemporal-MB BioSAR-1 sampling pattern, is reported in Fig. 1 for near range geometry. Here and in the sequel the deformation velocity is reported in terms of temporal frequency in phase cycles per month, and image intensity codes amplitude. Rayleigh/Fourier resolution limits are about 19 m for height and 0.5 cycles/month for temporal frequency, and strong sidelobes (ambiguities) are present due to
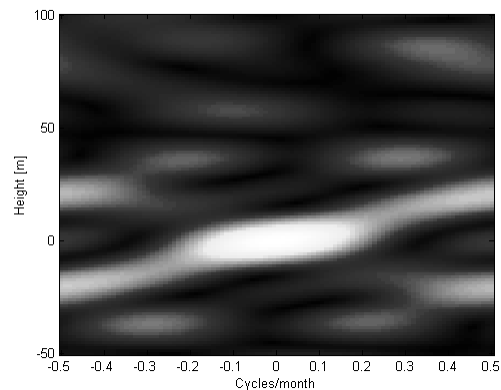

Figure 1 PSF in the height-velocity (temporal frequency) plane for the BIOSAR-1 multitemporal-multibaseline sampling pattern.

the sparse baseline-time sampling.

In Figs. 2-4 the moduli of the components of the scattering mechanisms $\hat{\mathbf{k}}(h,v)$ obtained in the Pauli basis are shown for three different cells. The multilook cell projected in ground is a square with side 50m, corresponding to some tens of looks. Scattering mechanisms have been represented with the classical Pauli basis RGB colour coding, and the image-intensity coded amplitude refers to the polarimetric total power [6-12]. The red channel corresponds to even bounce scattering components, the blue channel to the odd bounce ones, and the green channel typically to those due to random volumes (e.g. forest canopy) [2]. In Fig. 2, the scattering mechanisms have been estimated for varying h,v in a cell in near range containing a trihedral corner reflector located approximately at zero height; as expected, it appears coloured in blue. No significant ground deformation velocity is detected, as reasonable in this first test scenario. Also,

low ambiguities and a height-velocity superresolution can also be noted compared to the PSF of Fig. 1, thanks to an effective leakage reduction from the proposed filter for the Pol-Diff-Tomo operation. In Fig. 3, the scattering mechanisms in the height-velocity plane are imaged for a bare soil cell. The ground scatterer response is around zero height and zero velocity, and it is again coloured in blue, correctly corresponding to the single bouncing. Moreover, Fig. 4 shows the Pol-Diff-Tomo estimates for a two superimposed scatterers case (a forested cell). The ground scatterer (located at a height of about 10m) is apparently characterized by both a double bouncing (due to the electromagnetic interaction between ground and tree trunks) and single bouncing effects (bare soil); this is reasonable in the multilook scenario. Above the ground, it is possible to recognize the contribution of the canopy, behaving as a random volume triggering the channel coded in green. The response of both scatterers is again around the null velocity as expected.

For a second check of the motion detection capabilities of the new Pol-Diff-Tomo processing, a synthetic motion corresponding to a temporal frequency of -0.06 phase cycles per month has been injected into the real data to emulate a quick subsidence. This has been carried out for the cells used in Fig. 2 and Fig. 4. The Pol-Diff-Tomo result for the corner reflector cell is reported in Fig. 5; apparently, the scatterer response is at a temporal frequency resembling the synthetic injected value. The injected motion is also revealed in Fig. 6 showing the result for the two superimposed scatterers cell. The capability is confirmed of Pol-Diff-Tomo of jointly resolving heights, estimating deformation velocities, and characterizing the polarimetric scattering mechanism of multiple scatterers.

As a final proof of concept, Figs. 7 and 8 show Pol-Diff-Tomo results for a second corner reflector cell and a second bare soil cell, respectively, with no motion injected; good height, velocity and polarimetric signatures are apparent as in the previous results. Future work will regard performance analyses of this new coherent SAR data combination mode.
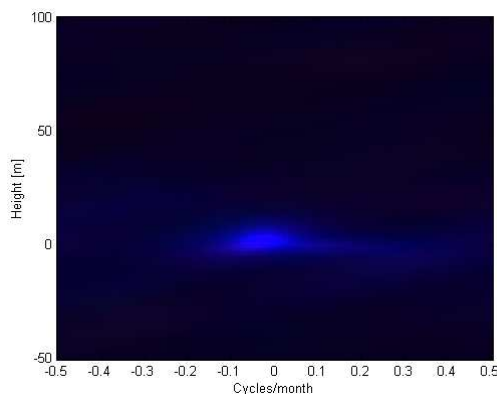
Figure 3 Pol-Diff-Tomo estimated scattering mechanisms in the height-velocity plane, bare soil cell, Pauli basis. Pauli colour coding is the same of Fig. 2.

Figure 4 Pol-Diff-Tomo estimated scattering mechanisms in the height-velocity plane, forested cell. Pauli basis colour coding.

Figure 2 Estimated scattering mechanisms in the height-velocity plane with the proposed Pol-Diff-Tomo processor, corner reflector, Pauli basis (Red: HH-VV, even bounce; Green: 2*HV, random volume; Blue: HH+VV, odd bounce).
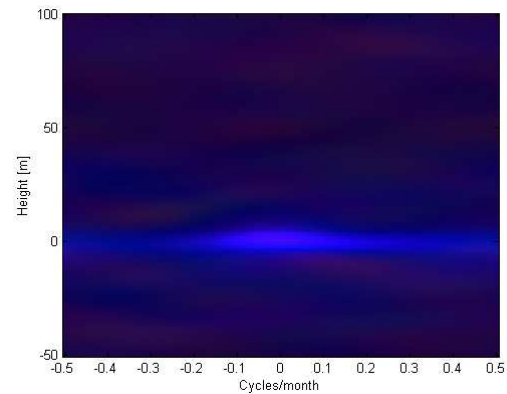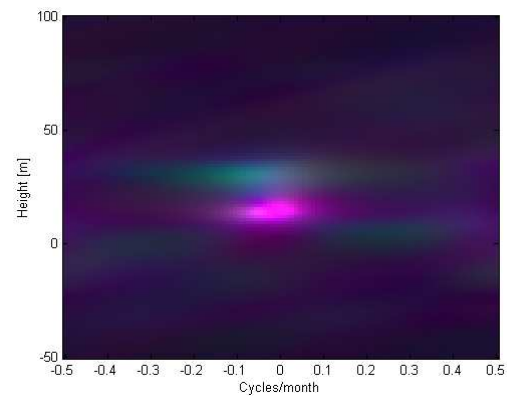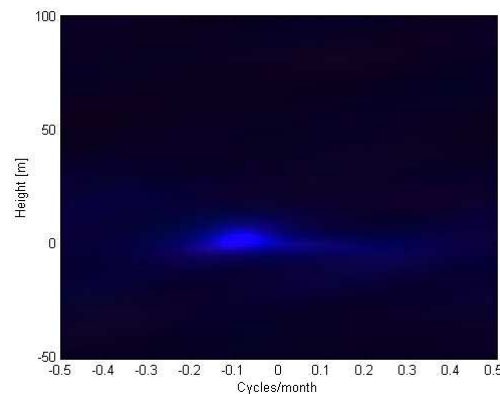
Figure 5 Pol-Diff-Tomo estimated scattering mechanisms in the height-velocity plane, corner reflector of Fig.2 with synthetic motion. Pauli coding.
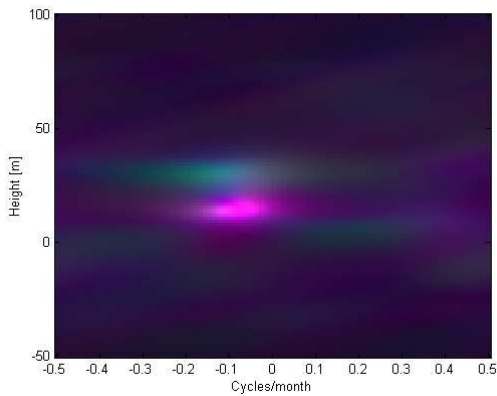
Figure 6 Pol-Diff-Tomo estimated scattering mechanisms in the height-velocity plane, forested cell of Fig. 4 with synthetic motion. Pauli coding.
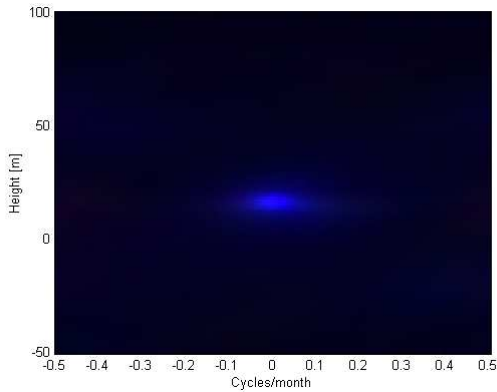

Figure 7 Pol-Diff-Tomo scattering mechanisms in the height-velocity plane, second corner reflector. Pauli coding.
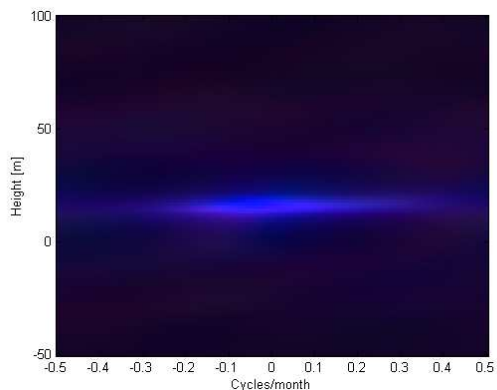

Figure 8 Pol-Diff-Tomo scattering mechanisms in the height-velocity plane, second bare soil cell. Pauli coding.

Acknowledgement

References

[1] S. R. Cloude, K. P. Papathanassiou: *Polarimetric SAR Interferometry*. IEEE Trans. on Geosci. Remote Sensing, vol. 36, pp. 1551-1565, Sept. 1998.

[2] A. Reigber, A. Moreira: *First Demonstration of Airborne SAR Tomography Using Multibaseline L-band Data*. IEEE Trans. on Geosci. Remote Sens., vol. 38, no. 5, pp. 2142-2152, May 2000.

[3] R.N. Treuhaft, B.E. Law, G.P. Asner, S. Hensley: *Vegetation Profile Estimates from Multialtitude, Multifrequency Radar Interferometric and Polarimetric Data*. Proc. IEEE Int. Geosci. and Remote Sens. Symp., July 2000.

[4] S. Tebaldini, F. Rocca, A. M. Guarnieri: *Model Based SAR Tomography of Forested Areas*. Proc. IEEE Int. Geosci. and Remote Sens. Symp., Boston, MA, USA, Jul. 2008.

[5] F. Lombardini, M. Pardini, G. Fornaro, *et al.*: *Linear and Adaptive Spaceborne Three-Dimensional SAR Tomography: A Comparison on Real Data*. IET Radar, Sonar and Navigation, vol. 3, no. 4, pp. 424-436, Aug. 2009.

[6] S. Sauer, L. Ferro-Famil, A. Reigber, *et al.*: *Multi-Aspect POL-InSAR 3D Urban Scene Reconstruction at L-Band*. Proc. of 2008 European SAR Conference, Friedrichshafen, May 2008.

[7] A. Ferretti, C. Prati, F. Rocca: *Nonlinear Subsidence Rate Estimation using Permanent Scatterers in Differential SAR Interferometry*. IEEE Trans. on Geosci. Remote Sensing, vol. 38, no. 5, pp. 2202–2212, Sept. 2000.

[8] P. Berardino, G. Fornaro, R. Lanari, E. Sansosti: *A New Algorithm for Surface Deformation Monitoring based on Small Baseline Differential SAR Interferograms*. IEEE Trans. on Geosci. Remote Sensing, vol. 40, no. 11, pp. 2375-2383, Nov. 2002.

[9] F. Lombardini: *Differential Tomography: A New Framework for SAR Interferometry*. IEEE Trans. Geosci. Remote Sens., vol. 43, no. 1, pp. 37-44, Jan. 2005.

[10] G. Fornaro, F. Serafino, D. Reale: *4D SAR Imaging for Height Estimation and Monitoring of Single and Double Scatterers*. IEEE Trans. on Geosci. Remote Sensing, vol. 47, no.1, pp.224-237, Jan.2009.

[11] F. Lombardini, M. Pardini: *Multiple Scatterers Identification in Complex Scenarios with Adaptive Differential Tomography*. Proc. IEEE Int. Geosci. and Remote Sens. Symp., Cape Town, South Africa, Jul. 2009.

[12] F. Lombardini, M. Pardini: *Experiments of 3D SAR Tomography Techniques With P-Band Polarimetric Data*. Proc. of 2009 ESA PolInSAR Workshop, Frascati, Italy, Jan. 2009.